# Fifteen terawatt picosecond $CO_2$ laser system

**D. Haberberger,* S. Tochitsky, and C. Joshi**

*Neptune Laboratory, Department of Electrical Engineering, University of California Los Angeles, 420 Westwood Plaza, Los Angeles 90095, California, USA*

**dhaberberger@ucla.edu*

**Abstract:** The generation of a record peak-power of 15TW (45J, 3ps) in a single $CO_2$ laser beam is reported. Using a master oscillator–power amplifier laser system, it is shown that up to 100J of energy can be extracted in a train of 3ps laser pulses separated by 18ps, a characteristic time of the $CO_2$ molecule. The bandwidth required for amplifying the short injected laser pulse train in a 2.5atm final $CO_2$ amplifier is provided by field broadening of the medium at intensities of up to 140GW/cm$^2$. The measured saturation energy for 3ps pulses is 120mJ/cm$^2$ which confirms that energy is simultaneously extracted from six rovibrational lines.



**OCIS codes:** (140.3470) Lasers, carbon dioxide; (020.2649) Strong field laser physics; (020.6580) Stark effect.

## Reference and Links

1. V. Yanovsky, V. Chvykov, G. Kalinchenko, P. Rousseau, T. Planchon, T. Matsuoka, A. Maksimchuk, J. Nees, G. Cheriaux, G. Mourou, and K. Krushelnick, "Ultra-high intensity- 300-TW laser at 0.1 Hz repetition rate," Opt. Express **16**(3), 2109–2114 (2008).
2. I. Pogorelsky, P. Shkolnikov, M. Chen, A. Pukhov, V. Yakimenko, P. McKenna, D. Carroll, D. Neely, Z. Najmudin, L. Willingdale, D. Stolyarov, E. Stolyarova, and G. Flynn, "Proton and ion beams generated with picosecond CO2 laser pulses," in Proceedings of Advanced Accelerator Concepts: 13th Workshop, W. Leemans, ed. (2009), pp. 532–537.
3. S. Ya. Tochitsky, C. Filip, R. Narang, C. E. Clayton, K. A. Marsh, and C. Joshi, "Efficient shortening of self-chirped picosecond pulses in a high-power CO(2) amplifier," Opt. Lett. **26**(11), 813–815 (2001).
4. S. Ya. Tochitsky, R. Narang, C. Filip, C. E. Clayton, K. A. Marsh, and C. Joshi, "Generation of 160-ps terawatt-power CO(2) laser pulses," Opt. Lett. **24**(23), 1717–1719 (1999).
5. P. B. Corkum, "Amplification of picosecond 10μm pulses in multiatmosphere $CO_2$ lasers," IEEE J. Quantum Electron. **21**(3), 216–232 (1985).
6. R. K. Brimacombe, and J. Reid, "Accurate measurements of pressure-broadened linewidths in a transversely excited $CO_2$ discharge," IEEE J. Quantum Electron. **19**(11), 1668–1673 (1983).
7. S. H. Autler, and C. H. Townes, "Stark effect in rapidly varying fields," Phys. Rev. **100**(2), 703–722 (1955).
8. R. K. Brimacombe, and J. Reid, "Influence of the dynamic Stark effect on the small-signal gain of optically pumped 4.3- μm $CO_2$ lasers," J. Appl. Phys. **58**(3), 1141–1145 (1985).
9. R. K. Brimacombe, and J. Reid, "Measurements of anomalous gain coefficients in transversely excited $CO_2$ lasers," IEEE J. Quantum Electron. **19**(11), 1674–1679 (1983).
10. V. T. Platonenko, and V. D. Taranukhin, "Coherent amplification of light pulses in media with a discrete spectrum," Sov. J. Quantum Electron. **13**(11), 1459–1466 (1983).
11. A. E. Siegman, *Lasers* (University of Science Books, Mill Valley, 1986).
12. A. J. Alcock, and P. B. Corkum, "Ultra-fast switching of infrared radiation by laser-produced carriers in semiconductors," Can. J. Phys. **57**, 1280–1290 (1979).
13. C. V. Filip, R. Narang, S. Y. Tochitsky, C. E. Clayton, and C. Joshi, "Optical Kerr switching technique for the production of a picosecond, multiwavelength $CO_2$ laser pulse," J. Appl. Opt. **41**(18), 3743–3747 (2002).
14. J.-M. Liu, *Photonic Devices* (Cambridge Univ. Press, 2005).
15. R. A. Ganeev, A. I. Ryasnyanskiĭ, and H. Kuroda, "Nonlinear optical characteristics of carbon disulfide," Opt. Spectrosc. **100**(Spec.), 108–118 (2006).
16. R. L. Carlson, J. Carpenter, D. Casperson, R. Gibson, R. Godwin, R. Haglund, J. Hanlon, E. Jolly, and T. Stratton, "Helios: a 15 TW carbon dioxide laser-fusion facility," IEEE J. Quantum Electron. **17**(9), 1662–1678 (1981).
17. B. F. Kuntsevich, V. O. Petukhov, S. Y. Tochitskiĭ, and V. V. Churakov, "Field mechanism for simultaneous oscillation on several transitions in TEA $CO_2$ lasers," Quantum Electron. **23**(6), 481–487 (1993).
18. S. Ya. Tochitsky, *et al*., "Present status and future prospects of high-power $CO_2$ laser research," in Proceedings of the International Conference LASERS 2000, V. J. Corcoran and T. A. Corcoran, eds. (2001), pp. 417–427.

#129173 - $15.00 USD Received 28 May 2010; revised 12 Jun 2010; accepted 15 Jun 2010; published 4 Aug 2010

19. L. M. Frantz, and J. S. Nodvik, "Theory of Pulse Propagation in a Laser Amplifier," J. Appl. Phys. **34**(8), 2346–2349 (1963).
20. D. Fröhlich, R. Wille, W. Schlapp, and G. Weimann, "Two-photon magnetoabsorption in multiple quantum wells," Phys. Rev. Lett. **61**(16), 1878–1881 (1988).
21. P. B. Corkum, P. P. Ho, R. R. Alfano, and J. T. Manassah, "Generation of infrared supercontinuum covering 3-14 microm in dielectrics and semiconductors," Opt. Lett. **10**(12), 624–626 (1985).
22. D. Haberberger, *et al*., "Proton acceleration in $CO_2$ laser plasma interactions at critical density," in Proceedings of Partical Accelerator Conference, Vancouver (2009).

## 1. Introduction

Chirped-pulse amplification (CPA) in large bandwidth media, such as Ti-Sapphire and Nd:Glass, has made it possible to achieve TW-PW powers in sub-picosecond pulses around 1μm wavelength [1]. Certain laser-particle and laser-plasma interactions would benefit from an ultra high-power mid-infrared source. For example, the quadratic wavelength scaling of the ponderomotive force can be beneficial in particle acceleration by a laser pulse [2]. Also, the use of relativistic 10μm pulses allows one to probe overdense plasma in the plasma density range of $n_e$ = 1-100$n_{cr}$ (where $n_{cr} = 1.1\text{x}10^{21}/\lambda^2[\mu\text{m}]\text{cm}^{-3}$) using visible frequency probes. For this wavelength region, $CO_2$ lasers are the only viable option for the production of high-power laser pulses. Even though high damage threshold of the gas medium (ionization) allows for non-CPA schemes, progress on 10μm picosecond pulse amplification to high power has been modest [2–4].

The main difficulty with building ultra-short $CO_2$ laser systems is that the gain spectrum is modulated with a molecular rotation structure that hinders the amplification of picosecond pulses. One method to circumvent this limitation is to operate the laser at multi-atmospheric gas pressures which increases the bandwidth of the spectral lines via particle collisions. In 1985, Corkum demonstrated this principle for the first time producing picosecond $CO_2$ laser pulses at the milijoule level through amplification in a 10atm laser [5]. Recently this technique has been used to reach powers up to 1TW in a 6ps pulse in the 10atm BNL $CO_2$ laser [2]. However, high pressure imposes a limitation on the aperture of the gain module in sustaining a stable electrical discharge.

Field broadening is an alternative method of obtaining sufficient bandwidth in the $CO_2$ molecule to support amplification of picosecond pulses. Here, the resonant interaction of the strong electric field of the laser pulse with the $CO_2$ molecule (similar to the ac Stark effect) causes an increase in the bandwidth. In this so-called "coherent amplification" regime, picosecond pulses may be amplified efficiently at lower pressures allowing the use of large-aperture lasers. In an earlier study we showed that terawatt 40ps pulses can be obtained in a 2.5atm $CO_2$ amplifier at an intensity of $10^{10}\text{W/cm}^2$, although the collisional bandwidth-limited pulse duration is 250ps [3]. Here, we report on the production of 10μm picosecond pulses with an unprecedented peak power of 15TW in the UCLA Neptune Laboratory $CO_2$ laser system. Strong field broadening at intensities of $10^{11}\text{W/cm}^2$ provides sufficient bandwidth for the amplification of 3ps pulses at a pressure of 2.5atm. The dynamics of a picosecond pulse train during the process of amplification in the $CO_2$ gain medium are described.

## 2. Theory and simulations of picosecond pulse amplification

### *2.1 $CO_2$ amplification with pressure broadening*

Conventional $CO_2$ lasers operated at atmospheric pressure lack sufficient bandwidth to amplify picosecond pulses. For example, on the 10P vibrational-roatational manifold, the gain spectrum at 1atm consists of discrete rotational transitions separated by 55GHz each having a bandwidth of ~3.7GHz (gas mix of 1:1:14 $CO_2$:$N_2$:He). This bandwidth limits the amplification to ~3ns pulses. The amplification of sub-ns pulses is made possible by the linear increase in rotational line bandwidth with the pressure of the $CO_2$ laser medium. The collisional bandwidth of the rotational line is related to the pressure of the gain medium according to the following equation [6]:

#129173 - $15.00 USD Received 28 May 2010; revised 12 Jun 2010; accepted 15 Jun 2010; published 4 Aug 2010

$$\Delta\nu_{pressure} = P \cdot \left(5.79\Psi_{CO_2} + 4.25\Psi_{N_2} + 3.55\Psi_{He}\right), \quad (1)$$

where $\Delta\nu_{pressure}$ is the pressure broadened rotational line bandwidth in GHz, P is the pressure of the $CO_2$ gas in atm, and $\Psi_a$ is the fraction of gas $a$ in the mixture. In Fig. 1 we show the calculated gain spectrum for the 10P branch of the 00°1-10$^0$0 vibrational band of the $CO_2$ molecule. These calculations have been done for three pressures: 1, 10, and 25atm.

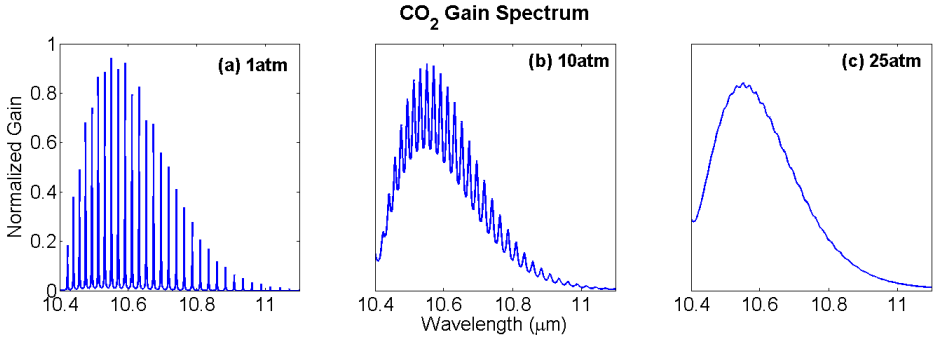


Fig. 1. $CO_2$ gain spectrum vs. wavelength with a gas mixture of 1:1:14 ($CO_2$:$N_2$:He) at a pressure of 1atm (a), 10atm (b), and 25atm (c)

Pressure broadening at 10atm (Fig. 1b) results in a 37GHz linewidth causing an overlap between neighboring rotational lines. Ideally, one would increase the pressure until a continuous spectrum is obtained across the entire vibrational branch spanning 1.2THz, which happens at ~25atm (Fig. 1c). Although with such a bandwidth picosecond pulses can be amplified in a straightforward manner, these pressures are not achievable in a discharge pumped system.

At realistic pressures (~10atm), picosecond pulses can still be amplified by seeding a pulse with a spectrum that covers multiple rotational lines. In this case, the seed spectrum (assumed to be a smooth Gaussian) is filtered through amplification by the gain spectrum which has a modulation at 55GHz (Fig. 1b). The resultant temporal structure of the pulse can be found through a Fourier transform of the gain filtered pulse spectrum that results in a pulse train of picosecond pulses separated by 1/55GHz = 18ps. This process is similar to mode locking. In the mode locking of an oscillator, many longitudinal modes locked in phase constructively interfere at a temporal separation of 1/(free spectral range), thus producing a pulse train output. Similarly in a $CO_2$ amplifier, the rotational lines are locked in phase by stimulation from the seed pulse and therefore their radiation will interfere to form a pulse train with a temporal separation equal to 1/(line separation).

The relationships between the spectral and temporal properties of the resultant pulse train are illustrated in Fig. 2 which shows the interaction between the spectra of a 3ps pulse and a 5atm $CO_2$ medium with a gas mix of 1:1:14 ($CO_2$:$N_2$:He). Figure 2a shows the $CO_2$ gain spectrum (red), the 3ps input pulse spectrum (green), and the pulse spectrum filtered by the $CO_2$ gain spectrum obtained via multiplication of the red and green traces (blue). The Fourier transform of the latter produces the expected temporal structure of the pulse after spectral filtering from the gain medium, shown in Fig. 2b. Three conclusions can be made by analyzing the data in Fig. 2. First, a pulse train is produced and has an expected pulse separation of 18ps. Second, the pulse duration of 3ps is preserved because the minimum pulsewidth is limited by the bandwidth of the whole 10P vibrational branch (1.2THz). Third, the width of the pulse train envelope (54ps) is estimated by the inverse of the individual spectral linewidth (18.5GHz). Note that similar pulse trains of 3ps $CO_2$ laser pulses were observed in autocorrelation measurements performed by P. Corkum [5].

#129173 - $15.00 USD Received 28 May 2010; revised 12 Jun 2010; accepted 15 Jun 2010; published 4 Aug 2010

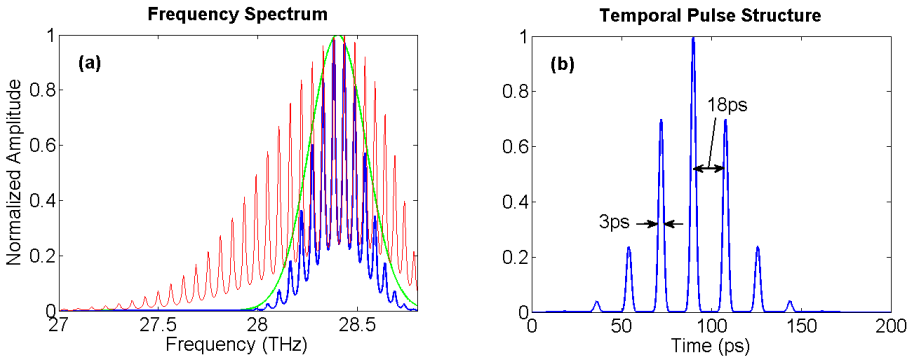


Fig. 2. (a) $CO_2$ gain spectrum at 1atm (red), 3ps input pulse spectrum (green), and the pulse spectrum filtered by the $CO_2$ gain spectrum obtained via multiplication of the red and green traces (blue). (b) Fourier transform of the pulse spectrum filtered by the $CO_2$ gain medium.

Although 3ps pulse trains can be produced and amplified in a pressure broadened $CO_2$ medium, there are two drawbacks in terms of high-power production. First, energy extraction in a high-pressure $CO_2$ laser is limited because of the restriction on the gas discharge aperture size. Second, even at the highest pressures achievable, the gain spectrum still exhibits an undesirably strong modulation at 55GHz that results in the distribution of the extracted energy over 50-100ps pulse train instead of a single 3ps pulse.

*2.2 Field broadening and pulse train evolution*

In addition to pressure broadening, the electric field of the laser pulse itself will broaden the bandwidth of the rotational lines due to the ac Stark Effect [7], a process commonly known as field broadening. The amount of spectral broadening is only limited by the intensity of the laser pulse and the ionization threshold of the gas, therefore it could potentially produce a continuous bandwidth across the entire vibrational branch.

The effect of field broadening on the rotational line bandwidth can be estimated by the following equation [8]:

$$\Delta\nu_{rot} = \Delta\nu_{pressure} + \Delta\nu_{field} = \Delta\nu_{pressure} + 2\cdot\Omega = \Delta\nu_{pressure} + 2\cdot\left(6.91\cdot10^{6}\,\mu\sqrt{I}\right), \quad (2)$$

where $\Delta\nu_{rot}$ is the total bandwidth of the rotational line, $\Delta\nu_{pressure}$ and $\Delta\nu_{field}$ are the contributions from pressure (Eq. (1)) and field broadening respectively, $\Omega$ is the Rabi frequency, $\mu$ is the dipole moment in Debye, and $I$ is the laser pulse intensity in W/cm$^2$. For the 10.6μm lasing transition, the dipole moment is equal to 0.0371 Debye [9]. Calculations using Eq. (2) show that at an intensity of 5GW/cm$^2$ for a 1atm amplifier, the resultant bandwidth of 37GHz is comparable to that of a 10atm amplifier (see Fig. 1b). Therefore, with a sufficiently intense 10μm pulse, field broadening can compensate for the lack of bandwidth in low pressure amplifiers.

The production of a pulse train in the early stages of amplification is inevitable because of the residual 55GHz modulation in the gain spectrum at practical operating pressures. Therefore, it is important to study the effect of field broadening on the amplification of a pulse train where the bandwidth is continually increasing due to increasing intensity as the pulse is amplified. For this purpose, we have used a simulation code written by V. Platonenko [10] to model the amplification of a pulse train in the presence of field broadening. The results of the simulation are presented in Fig. 3 which displays the intensity distribution of the pulse train at various stages of the amplification defined by the $g_oL$ product, where $g_o$ is the small signal gain of the amplifier and L is the length.

#129173 - $15.00 USD Received 28 May 2010; revised 12 Jun 2010; accepted 15 Jun 2010; published 4 Aug 2010

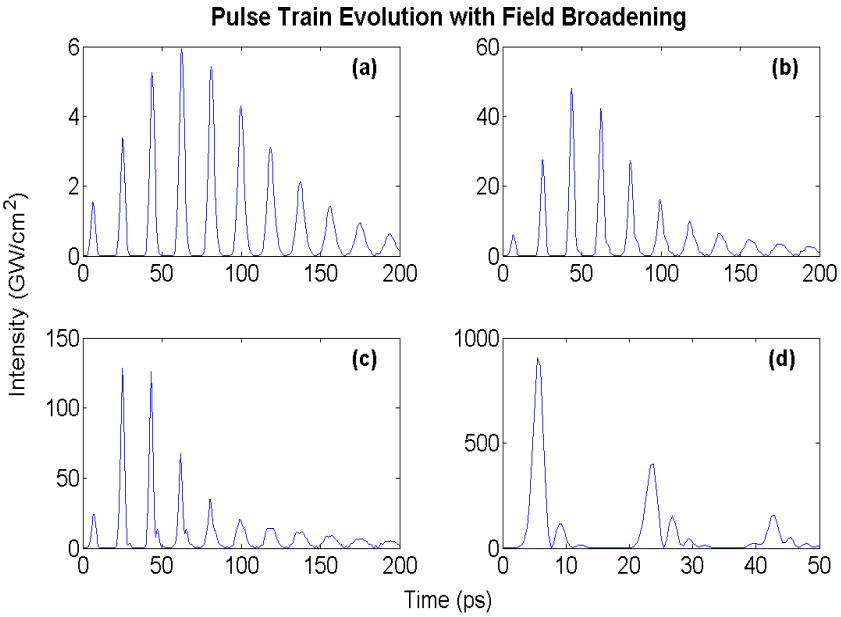


Fig. 3. Pulse train evolution shown through consecutive plots of intensity vs. time as the pulses travel through a $CO_2$ amplifier at a pressure of 3atm with a small signal gain of go = 3%/cm. (a), (b), (c), and (d) are taken at $g_oL$ products of 6.4, 9.6, 12.8, and 25.6 respectively.

In this simulation, a 3atm module is used to amplify a 3ps pulse with an input intensity of 100MW/cm$^2$. At this level of intensity, lack of field broadening in a low-pressure amplifier leads to the production of a pulse train as seen in Fig. 3a. However, as the intensity increases from 6 to 125GW/cm$^2$ (Fig. 3a-c), a significant shortening of the pulse train is observed. As the field broadened bandwidth increases, the extracted energy is distributed over a proportionally decreasing number of pulses. Further amplification to 900GW/cm$^2$ (Fig. 3d) results in ~60% of the extracted energy in the first pulse. At this intensity, the onset of Rabi Flopping of the lasing transition [11] is seen to occur and effectively shortens the pulsewidth of the individual pulses. Ultimately, at even higher intensities, amplification in a relatively low-pressure $CO_2$ amplifier will evolve a pulse train into a single pulse.

Generation of high-power 10μm pulses in a $CO_2$ laser chain must then involve the use of both pressure and field broadening. A high power picosecond $CO_2$ laser system should have two stages of amplification. The first stage amplifies a nJ level seed pulse to the mJ level in a pressure broadened regime. This results in a pulse train whose envelope is restricted by the pressure broadened bandwidth of the individual rotational line. In the second stage of amplification, the mJ level pulse train is amplified to the Joule level in low-pressure, large-aperture amplifiers where the field broadening mechanism assists in the evolution of the pulse train into a single pulse. This strategy is the basis behind the multi-terawatt $CO_2$ laser chain in the Neptune Laboratory described below.

## 3. Experiments

The $CO_2$ master oscillator – power amplifier (MOPA) laser system based in the Neptune Facility at UCLA is shown schematically in Fig. 4. It is based on the production of a 3ps 10μm seed pulse which is regeneratively amplified in a high-pressure preamplifier from a nJ to the mJ level, and then injected into a final 2.5atm amplifier to give an output energy of ~100J in a pulse train.

#129173 - $15.00 USD Received 28 May 2010; revised 12 Jun 2010; accepted 15 Jun 2010; published 4 Aug 2010

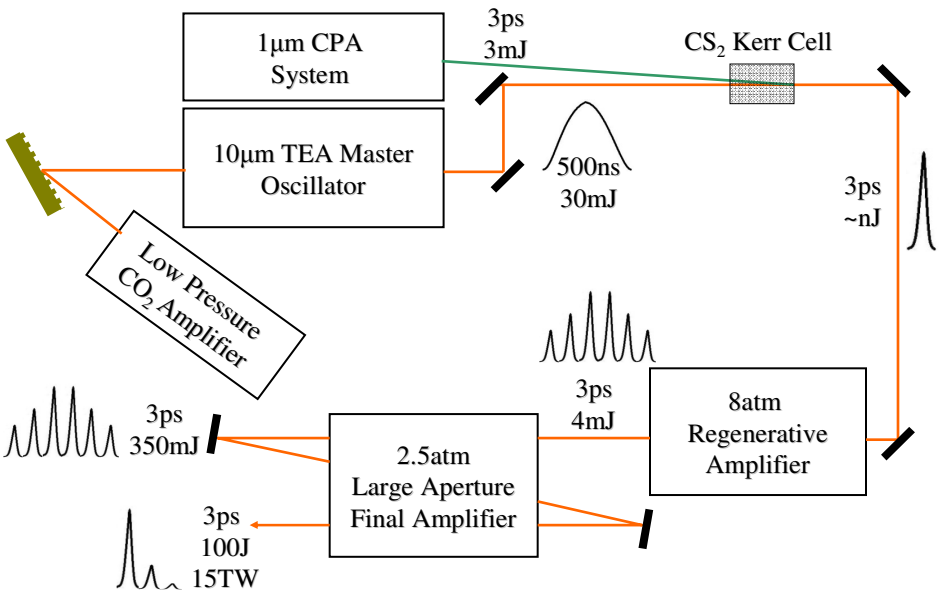


Fig. 4. The Neptune $CO_2$ master-oscillator power-amplifier laser chain

*3.1 Short 10μm seed production*

There are various methods by which a picosecond 10μm seed pulse can be generated using a short 1μm pulse, the most common of which is semiconductor switching [12]. An alternative method makes use of the ability of the short intense 1μm pulse to gate the 10μm radiation using the Kerr effect [13]. In mediums that exhibit the optical Kerr effect, the index of refraction is dependent on the intensity of an optical pulse according to the following [14]:

$$n(I) = n_o + n_2 I, \tag{3}$$

where $n_o$ is the linear index of refraction, $n_2$ represents the strength of the Kerr effect in the medium, and $I$ is the intensity of the pump pulse in W/cm$^2$. This change of the refractive index along the polarization axis of the pump pulse induces a birefringence in the medium which can be used as a transient phase retarder for a weaker 10μm pulse. To obtain full 90° rotation of the 10μm polarization, the following equation must be satisfied [14]:

$$\left| n(I) - n_o \right| = \frac{\lambda}{2d}, \tag{4}$$

where $n(I)$ is the index of refraction according to Eq. (3), $\lambda = 10\mu m$, and $d$ is the length of the Kerr medium.

The Kerr medium chosen is carbon disulfide, $CS_2$, due to its transparency at 10μm (1μm) and large nonlinear refractive index of $n_2 = 2\text{x}10^{-14}$cm$^2$/W [15]. Group velocity dispersion in $CS_2$ between the wavelengths of the pump pulse (1μm) and the probe pulse (10μm) is 1ps/cm, therefore the length of our Kerr cell is limited to 1cm to avoid broadening of the 10μm seed pulse. For the above stated parameters, 90° rotation is provided with an intensity of 25GW/cm$^2$, a practical value for picosecond pulses.

An Nd:glass 1μm CPA system was built for controlling the $CS_2$ Kerr switch. A GLX-200 glass oscillator produces 500fs pulses which are stretched to ~1ns in a grating stretcher. The pulses are then amplified in a glass regenerative amplifier and two single-pass booster amplifiers to ~4mJ. Finally the pulses are compressed down to 3ps containing 3mJ.

#129173 - $15.00 USD Received 28 May 2010; revised 12 Jun 2010; accepted 15 Jun 2010; published 4 Aug 2010

Approximately 1mJ of the energy is split off from the main beam and focused into the $CS_2$ Kerr cell with a spot size $w_o$ = 1mm producing an intensity of 10GW/cm$^2$. The rest of the 1μm is sent to a Ge semiconductor switch.

The 10μm pulse is produced by a hybrid TEA $CO_2$ oscillator. Single longitudinal mode output is obtained by placing a low pressure (30 Torr) amplifier in the cavity along with the TEA module. The output of the hybrid oscillator is 30mJ in a 500ns pulse. This pulse is copropagated with the 1μm pulse at a small angle (~2°) through the Kerr cell. The polarization of a 3ps portion of the 10μm pulse is rotated from s- to p-polarization and transmitted through a 6-plate Ge analyzer (II-VI Inc., model:PAG-15-AC-6) that provides a measured contrast of $5x10^5$. This measurement was carried out by comparing the throughput of the Ge analyzer with and without a λ/2 waveplate placed in front of the Kerr cell. After the analyzer, the $CO_2$ laser beam is sent to the 1μm controlled Ge semiconductor switch to increase the contrast. Here, the 1μm pulse forms a plasma on the surface of the Ge plate inducing reflection for 10μm radiation a few picoseconds before the arrival of the seed pulse. The aspect ratio of the overlapped beams on the Ge plate provided a Gaussian profile for the reflected 10μm pulse. Although the 1μm pump intensity is less than half that required for 90° rotation in the Kerr switch, the nJ level seed delivered to the regenerative amplifier is sufficient for injection mode locking of a high-pressure regenerative amplifier.

*3.2 Regenerative amplification*

The 3ps seed pulses are sent into an 8atm TE $CO_2$ laser for regenerative amplification. The laser has a gain volume of 1x1x60cm$^3$ and is filled with a gas mix of 1:1:14 ($CO_2$:$N_2$:$H_3$). The amplifier is injection mode locked by seeding through a 50% ZnSe output coupler. It therefore produces a pulse train with a separation equal to the 12ns cavity roundtrip time. The total gain of ~$10^7$ brings the ~nJ level seed pulse to ~10mJ. The injection mode locked pulse train is decoupled from the seed pulse vector via transmission through the Ge semiconductor switch after the decay of the surface plasma. The pulse with maximum energy (10mJ) is then switched out using an external Pockels cell placed between crossed polarizers. A total efficiency of ~40% for this single pulse selector results in a 4mJ seed pulse for the final amplification.

The temporal structure of the regeneratively amplified $CO_2$ pulses is measured with a Hammamatsu (C5689) streak camera. The spectral sensitivity of the streak camera peaks in the visible wavelength range; therefore, the 10μm light is up-converted to a red wavelength using a $CS_2$ Kerr switch. Here, the intense 10μm pulses are used as the pump pulse while the probe pulse is provided by a red diode laser. The switched out red light then carries the temporal structure of the 10μm pulse and is sent to the streak camera for measurement. One such measurement of the regeneratively amplified pulses is displayed in Fig. 5 where the production of a pulse train with an 18ps pulse separation is evident.

#129173 - $15.00 USD Received 28 May 2010; revised 12 Jun 2010; accepted 15 Jun 2010; published 4 Aug 2010

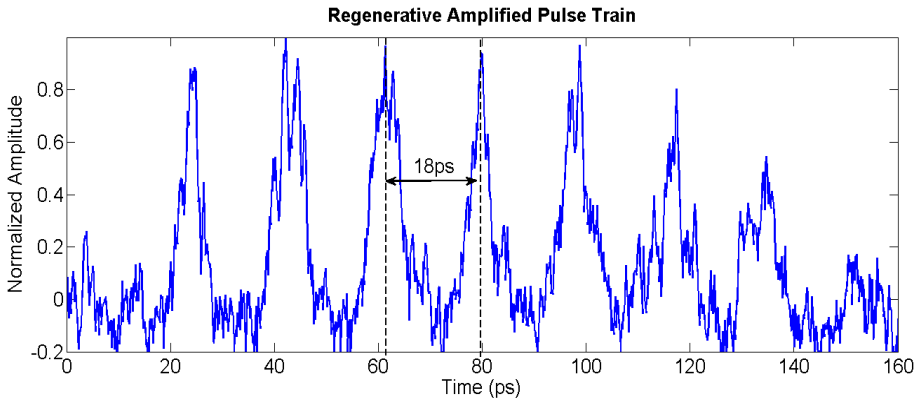


Fig. 5. Temporal profile of the $CO_2$ pulses after amplification in the regenerative amplifier as measured by the Hammamatsu (C5689) streak camera.

The expected individual pulsewidths of 3ps is near the resolution limit of the streak camera, therefore their mearsurement must take into account the instrumental function of the streak camera. The streak camera's instrumental function, or resolution, was experimentally determined to be 3ps via measurement of sub-picosecond 532nm laser pulses. In the streak camera measurements of the $CO_2$ amplified pulse, the actual pulse width is obtained by deconvolution using:

$$t_p^2 = t_m^2 - t_{ins}^2, \tag{5}$$

where $t_p$ is the actual pulsewidth, $t_m$ is the pulsewidth as measured by the streak camera, and $t_{ins}$ is the temporal resolution of the streak camera. The application of Eq. (5) to the measurement of the individual pulsewidths seen in Fig. 5 leads to an average temporal FWHM of 3.3ps. This measurement confirms that the vibrational branch bandwidth supports the amplification of ~3ps pulses.

The regenerative amplification produces a pulse train on the picosecond timescale due to the residual 55GHz modulation in the gain spectrum at 8atm. The length of the pulse train envelope at the output of the laser is governed by the pulse broadening equation [11]:

$$\tau_p^2(z) = \tau_p^2(0) + (16\ln 2)\ln G_o \big/ \Delta\omega^2, \tag{6}$$

where $\tau_p(0)$ and $\tau_p(z)$ are the initial and final FWHM of the pulse train envelopes, $G_o$ is the total gain, and $\Delta\omega$ is the gain bandwidth. In predicting the effect of pulse broadening on the width of the pulse train envelope, the restricting bandwidth is that of the rotational line. At 8atm $\Delta\omega/2\pi = 37GHz$, and for $\tau_p(0) = 3ps$ and $G_o = 10^7$, the expected gain narrowed pulse train envelope (FWHM) is ~60ps, which is in relative agreement with the ~100ps FWHM pulse train envelope seen in the streak camera measurements (Fig. 5).

*3.3 Final amplification*

The final amplification occurs in a large aperture (20x35cm) amplifier employing an electron-beam controlled discharge [16]. Three passes through the amplifier totaling 7.5m provide a gain of $G_o$~25,000 that produces 100J from the 4mJ seed. It is operated at 2.5atm with a gas mix of 4:1 ($CO_2$:$N_2$) resulting in a collisional line bandwidth of 14GHz. In the absence of further broadening, this bandwidth would result in an amplified pulse train envelope of 100's of picoseconds distributing the extracted energy into many pulses. However measurements of the amplified pulse train temporal profile recorded by the streak camera show a significant

#129173 - $15.00 USD Received 28 May 2010; revised 12 Jun 2010; accepted 15 Jun 2010; published 4 Aug 2010

shortening of the injected pulse train down to 2-3 pulses (Fig. 6b). The evolution from the seeded pulse train shown in Fig. 5 to the amplified pulse train in Fig. 6b is attributed to the significant increase in the $CO_2$ linewidth induced by field broadening and is in qualitative agreement with our simulation results displayed in Fig. 3. Note, due to an elevated jitter in the Hammamatsu streak camera, the single shot nature of the final amplifier necessitated the use of a Hadland Photonics (Imacon 500) streak camera with a temporal resolution of 5ps.

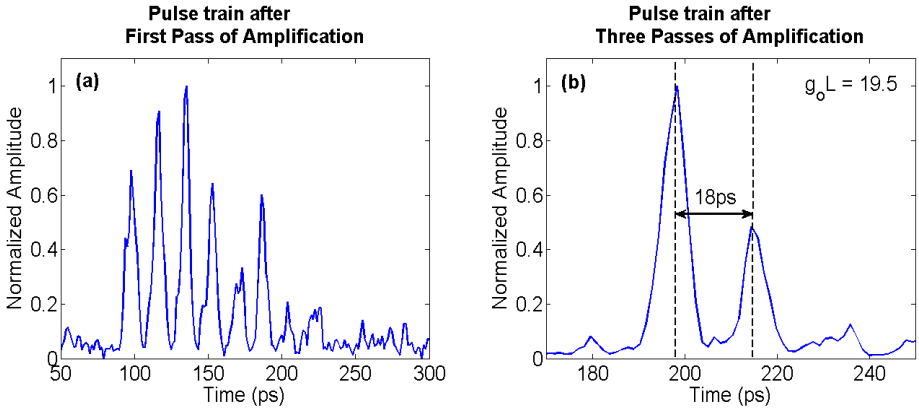


Fig. 6. Temporal profiles of the $CO_2$ pulses after amplification in the first pass of the final amplifier (a), and all three passes of the final amplifier (b) as measured by the Hadland Photonics (Imacon 500) streak camera.

The input beam for the first pass of amplification is quasi-collimated with a radius of $w_o$ = 4mm which provides an input intensity of only ~200MW/cm$^2$. At this low intensity, one would expect the lack of strong field broadening in a low-pressure amplifier to broaden the pulse train significantly. However, at a measured total gain of $G_o$~100 in the first pass, the pulse train broadening per Eq. (5) is only 15ps. The output of the first pass is sent to the streak camera diagnostic and based upon the temporal profile shown in Fig. 6a, no appreciable broadening has occurred.

In the second and third passes of amplification, the beam is expanded from a $w_o$ = 1cm to $w_o$ = 6.25cm to extract a large amount of energy and avoid laser damage of an NaCl window. The total gain of these passes is $G_o$~285 producing 100J from the input 350mJ. Using the energy partition extracted from the streak camera lineouts (Fig. 6a and 6b), this corresponds to an increase in peak intensity from 4GW/cm$^2$ to 140GW/cm$^2$. At these intensities field broadening can augment the 14GHz bandwidth of the 2.5atm amplifier to values up to ~200GHz. With such a bandwidth, one would expect the gain spectrum to be continuous across the entire vibrational branch. Thus, field broadening makes it possible to amplify high-power picosecond pulses in a low-pressure amplifier. A conservative estimation from Fig. 6b of the energy partition gives ~45J (45%) in the peak 3ps pulse, which equates to 15TW of power.

*3.4 Energy extraction in picosecond pulse amplification*

Efficient energy extraction is an important aspect of the production of high-power pulses. In $CO_2$ lasers, the energy of the gain medium is stored in a manifold of rotational levels with a Boltzmann distribution across the vibrational branch. For pulsewidths $t_p$>18ps, the spectrum of the pulse only directly interacts with a single rotational line. In this case, the saturation energy is related to the ratio of $t_p$ and $t_r$, the rotation relaxation constant (~100ps-atm). For $t_p$>>$t_r$, such as for nanosecond long pulses, the $CO_2$ molecule relaxation sustains a Boltzmann equilibrium between rotational lines which allows the laser pulse to extract energy from the entire vibrational branch. As $t_p$ is shortened and approaches $t_r$, as realized in the pressure broadened case, the "rotational bottleneck effect" prevents repopulating of the rotational laser

#129173 - $15.00 USD Received 28 May 2010; revised 12 Jun 2010; accepted 15 Jun 2010; published 4 Aug 2010

levels [17]. This causes the saturation energy to decrease and asymptotically approach that of a single line extraction, or 1/15th of the energy stored in the vibrational band. However, further decrease in the $t_p$ to less than 18ps results in the direct interaction between the pulse and multiple rotational lines separated by 55GHz. In this case, energy is simultaneously extracted from the lines contained within the input pulse bandwidth causing an increase in saturation energy. Ultimately, for a 1ps input pulse the stored energy from the entire vibrational branch can be extracted resulting in a saturation energy of 300mJ/cm$^2$ [18].

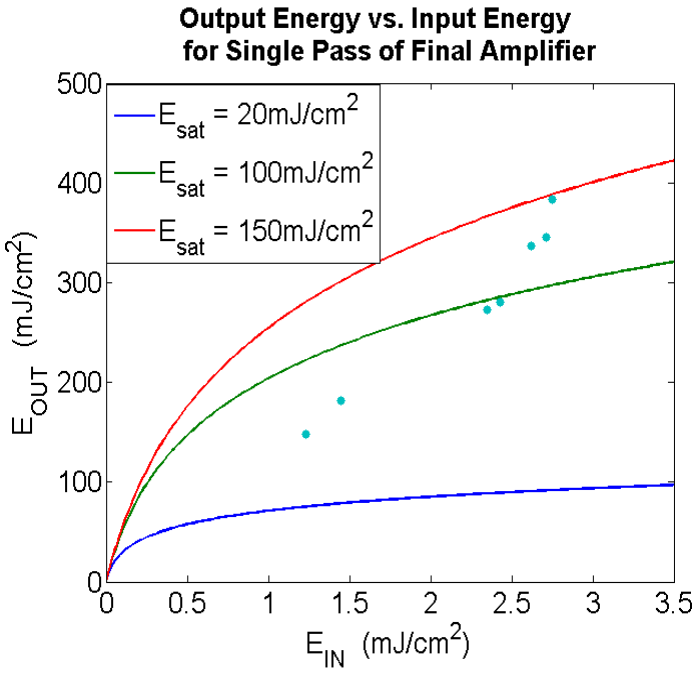


Fig. 7. Output energy vs. input energy from the first pass of the final amplifier (data points), compared to theoretical predictions of the Frantz Nodvik equation for a saturation energy of 20mJ/cm$^2$ (blue), 100mJ/cm$^2$ (green), and 150mJ/cm$^2$ (red)

As described in the previous section, amplification of a broadband 3ps pulse train in the first pass of the final amplifier is made with a quasi-collimated small beam. In the experiment we observed strong deviation from exponential growth by a factor of five as a result of strong saturation. Thus, in order to extract the saturation energy value, the output pulse energies from the first pass of amplification are measured while varying the amplitude of the input pulse. The results are plotted in Fig. 7 and compared to Frantz-Nodvik calculations [19] using a measured small signal gain of 2.6%/cm and gain length of 2.5m. From these results, we can extract a saturation energy of approximately 120mJ/cm$^2$. In previous measurements using 100ps pulses in the first pass of this amplifier resulted in a saturation energy of <20mJ/cm$^2$ [3]. This comparison shows a clear indication that the dynamics of the energy extraction has changed drastically between the amplification of 100ps and 3ps pulses. As opposed to the 100ps pulse that only directly interacts with a single rotational line, the 333GHz bandwidth of the 3ps pulse covers six rotational lines. Note that for a 100ps long pulse train used for the measurement, the rotational relaxation constant of 43ps in the amplifier introduces only a mall error in the saturation energy value. It is important to stress that this extracted value is in good agreement with the theoretical value for 3ps pulses [18].

#129173 - $15.00 USD Received 28 May 2010; revised 12 Jun 2010; accepted 15 Jun 2010; published 4 Aug 2010

## 4. Summary

We describe here a $CO_2$ master oscillator-power amplifier laser chain in which a 3ps, 10μm seed pulse is amplified to a peak power of 15TW. The total extracted energy reaches 100J and it is distributed over several 3ps pulses separated by 18ps, a time characteristic to the separation between the $CO_2$ molecule rotational lines. The formation and temporal dynamics of such a pulse train are fundamental properties of picosecond pulse amplification in a $CO_2$ active medium having a residual gain modulation. We show both experimentally and in simulations that significant shortening of the pulse train envelope results from amplification at high laser intensities of $10^{10}$-$10^{11}$W/cm$^2$. This shortening is attributed to an increase in the $CO_2$ molecule bandwidth due to the field broadening mechanism. This coherent amplification is realized in a 2.5atm large-aperture $CO_2$ module, thus opening possibilities to extract 100s of Joules of energy in picosecond pulses by using a low-pressure gas. An additional artifact of $CO_2$ laser amplification of picosecond pulses is an increase in energy extraction. This fact is shown by a six times increase in the measured saturation fluence of 20mJ/cm$^2$ for 100ps pulses to 120mJ/cm$^2$ for 3ps pulses. Energy extraction in the picosecond regime is very efficient because for a broadband pulse, energy is simultaneously extracted from multiple lasing transitions.

Simulations show that further amplification of the obtained pulses in the intensity range of $10^{11}$-$10^{12}$W/cm$^2$ induces Rabi flopping of the lasing transition. This leads to a significant shortening of the pulse from 3ps down to <1ps, which is accompanied with an increase in the saturation energy to 300mJ/cm$^2$. Realization of such a scheme would allow for the generation of 100TW and higher powers at 10μm in a single pulse, parameters unimaginable without coherent amplification.

Picosecond pulse amplification in $CO_2$ lasers can be also promising for applications where a high-repetition rate source is needed. Here, simple slicing of a TEA $CO_2$ laser output using a $CS_2$ Kerr switch enables one to obtain pulses as short as <100fs [15] providing ~1MW of power for nonlinear spectroscopy [20]. For high-power 10-100GW 10μm pulses, a conventional TEA $CO_2$ module can serve as a final amplifier accessing the ~1-3J energy range. Production of MW pulses in the 3-14μm range via supercontinuum generation [21] and development of a $CO_2$ laser driven ion source in a gas jet [22] are just two of many potential applications for a compact picosecond $CO_2$ laser system run at 1-10Hz.


## Acknowledgments

The authors would like to acknowledge Igor Pogorelsky (BNL) for constant interest and support for this work. This work was supported by DOE Contract No. DE-FG03-92ER40727.


#129173 - $15.00 USD Received 28 May 2010; revised 12 Jun 2010; accepted 15 Jun 2010; published 4 Aug 2010